www.czasopisma.pan.pl PAN POLSKA AKADEMIA NAUK www.journals.pan.pl

Arch. Metall. Mater. **63** (2018), 3, 1503-1507

DOI: 10.24425/123839

H.S. PARK*, I. SON*#

EFFECT OF Fe CONTENT ON THE CONTACT RESISTANCE OF ELECTROPLATED Au-Fe ALLOY LAYERS

In this study, variations in the contact resistance of electroplated Au-Fe alloy layers with Fe content were investigated. The contact resistance of electroplated Au-Fe alloy layers that were subject to thermal aging at 260°C in the atmosphere, tended to increase significantly with an increase in the Fe content. Through an analysis method employing X-ray photoelectron spectroscopy (XPS/ESCA) and Auger electron spectroscopy (AES), Ni oxides, such as NiO and Ni_2O_3, on the surface of the thermally aged electroplated Au-Fe alloy layers were observed. It is believed that the Ni oxide existing on the surface diffused from the underlying electroplated Ni layers to the surface through the grain boundaries in the electroplated Au-Fe layers during the thermal aging. As the Fe content in the electroplated Au-Fe layers increased, the grain size decreased. As the grain size decreases, more Ni oxide was detected on the surface. Therefore, with a rise in the Fe content, more Ni diffuses to the surface via grain boundaries, and more Ni oxide is formed on the surface of the electroplated Au-Fe layers, increasing the contact resistance of the electroplated Au-Fe alloy layers.

Keywords: Electroplating, Au-Fe alloy, Contact resistance, Thermal aging

1. Introduction

As electroplated gold alloy layers have an excellent resistance to corrosion and a low contact resistance, they are widely applied to the connection parts of electronic components such as connectors and printed circuit boards (PCBs) [1,2]. For connecting electronic components with high connection reliability, connective surfaces with a constant and low contact resistance in a given environment are required. The contact resistance between the electroplated gold alloy layers and the connective surfaces significantly varies depending on the type of alloy elements added, the thermal aging temperature, duration of the surface mounting process, and the type of underlayers. It has also been reported that the thermal aging undergone by the electroplated layers during the surface mounting process causes the surface diffusion of underlayer elements, thereby increasing the contact resistance [3-5]. Such an increase in contact resistance is expected to significantly vary depending on the temperature and duration of the thermal aging. Nickel and cobalt are mainly used as the alloy elements of electroplated gold alloy layers. The electrical properties of the layers, such as the contact resistance, can significantly vary depending on the type and contents of the alloy [6-8]. Recently, studies on the physical properties of electroplated Au alloy layers with iron (an iron group metal) as the alloy element, instead of nickel and cobalt, have been conducted [9,10]. Although the electroplated Au-Fe alloy layers reportedly have a lower internal stress than the conventional electroplated Au-Ni and Au-Co alloy layers, little is known about their contact resistance [11]. In addition, the alloy elements nickel and cobalt are known to be environmentally harmful substances that may cause skin allergies and cancers in humans [12]. Iron is therefore the most promising alloy element that can replace them.

As such, in this study, electroplated Au alloy layers were fabricated using iron as the alloy element, and the effect of Fe content on the contact resistance of the electroplated Au-Fe alloy layers after thermal aging was investigated. Furthermore, the contact resistance variation of the electroplated Au-Fe alloy layers as a function of Fe content after thermal aging was investigated using surface analysis methods such as X-ray photoelectron spectroscopy (XPS) and Auger electron spectroscopy (AES).

2. Experimental

Pure copper specimens with a 2 cm^2 surface area were used as the base materials. Nickel layers with approximately 2 μm thick were formed as underlayers using the electroplating method, and electroplated Au-Fe alloy layers of 0.15 μm in thickness were prepared. The thickness of the electroplated Au-Fe alloy layers was measured using an X-ray fluorescence plating thickness meter (XDLM-C4, Helmut Fisher, Germany). Pretreatment of the Cu specimens was performed in the following order: polishing, cathodic electrolytic degreasing, and acid dipping. The nickel undercoating was carried out using an electroplating solution, wherein an organic brightener (MAKROLUX-NF, ATOTECH, Germany) was added to a Watts bath to obtain a uniform glossy

* KYUNGPOOK NATIONAL UNIVERSITY, DEPARTMENT OF MATERIALS SCIENCE AND METALLURGICAL ENGINEERING, 80 DAEHAK-RO, BUK-GU, DAEGU, 41566, KOREA

Corresponding author: ijson@knu.ac.kr

appearance. The Au-Fe alloy electroplating was performed using different iron sulfate concentrations (0.22~14.28 mM) in the electroplating solutions whose compositions are listed in Table 1. Table 1 shows the conditions for the Au-Fe electroplating and the composition of the electroplating solution.

TABLE 1

Composition of the Au-Fe alloy electroplating solution and electroplating conditions

Potassium gold cyanide ($KAu(CN)_2$)	0.031 M
Citric acid ($C_6H_8O_7$)	0.260 M
Potassium citrate ($C_6H_5K_3O_7$)	0.277 M
Nitrilotriacetic acid ($C_6H_9NO_6$)	0.026 M
Ferrous sulfate heptahydrate ($FeSO_4 \cdot 7H_2O$)	0.22, 0.89, 3.57, 14.28 mM
pH	4.2
Temperature (°C)	40
Anode	Pt/Ti mesh
Current density (A/m^2)	50

To investigate the content of Fe present in the electroplated layers, a spectrophotometric determination analysis, using an inductively coupled plasma spectrophotometer (ICP-OES, Optima 7300DV, Perkin Elmer, USA), was conducted. For this analysis, a Ti plate (with a 20 cm^2 surface area) was electroplated for 30 min under the conditions described in Table 2. The electroplated layers were then peeled off, and the solution dissolved in aqua regia was used. Table 2 shows the Fe content in the electroplated layers according to the Fe concentration of the solution.

TABLE 2

Fe content in the electroplated Au-Fe alloy layers in relation to the Fe concentration of the electroplating solution

Fe concentration in the solution (mM)	**Fe content in the electroplated Au-Fe alloy (wt.%)**
0.22	0.11
0.89	0.18
3.57	0.31
14.28	0.52

Thermal aging of the gold alloy electroplated specimens was performed at 250°C for three and five minutes, using a hot plate (HHP-411V, Shamal hotplate, Japan) under atmospheric pressure. The contact resistance of the electroplated Au-Fe layers based on the load increase was measured in the order of 10 g, 25 g, 50 g, 75 g, and 100 g, using a direct current contact resistance meter (356H, Tsuruga, Japan). For each specimen, five measurements were made and the average contact resistance values for all the specimens were compared.

To investigate the variation of contact resistance with respect to Fe content, surface analysis was conducted using an X-ray photoelectron spectrometer (Quantera SXM, ULVAC-PHI, USA) and an Auger electron spectrometer (PHI 710 Scanning Auger nanoprobe, ULVAC-PHI, USA). A depth-wise quantitative analysis of the elements was conducted, and the chemical bonding state was investigated by performing an Ar ion etching. The Au-0.52 wt.% specimens, subjected to thermal aging for five minutes, were processed using a focused ion beam (Versa3D LoVac, FEI Company, Netherlands). A cross-section observation as well as an EDS component analysis was conducted using FE-TEM (Titan G2 ChemiSTEM Cs Probe, FEI Company, Netherlands). In addition, the grain size of the electroplated Au-Fe alloy layers was derived using the Scherrer equation [13] by an X-ray diffraction (D/Max-2500, Rigaku, Japan).

3. Results and discussion

The effect of thermal aging on the contact resistance of an Au-Fe alloy containing 0.11-0.52 wt.% Fe was investigated. The results are shown in Fig. 1. In the case of an Au-Fe alloy without thermal aging (a), a low contact resistance (20 mΩ or less) was obtained at 0.098-0.98 N loads. With an increase in Fe content, the contact resistance increased slightly. After thermal aging was performed for three minutes (b) and five minutes (c) in the atmosphere, the contact resistance significantly increased with the increase in Fe content. In addition, the contact resistance increased with the duration of thermal aging, from three to five minutes. However, in all specimens, the contact resistance decreased with increasing load. This is possibly due to an increase in the contact area between the surface of the electroplated layers and the probe. The contact resistance before thermal aging (a) showed little difference according to the Fe content. The contact resistance after thermal aging [(b) and (c)], however, showed a large difference with Fe content, and the difference significantly increased with increasing Fe content. The difference in the contact resistance further increased with increasing duration of thermal aging.

Figure 2 shows an XPS depth profile of the electroplated Au-0.18 wt.% Fe alloy layers that were subject to thermal aging in the atmosphere for five minutes. High contents of Ni and O were detected on the surface of the Au-Fe alloy layers where thermal aging was performed. Ni and O were barely present within the Au-Fe alloy layers, yet high concentrations were present on the surface. It could imply that Ni from the underlayer was diffused to the surface of the Au-Fe alloy layers by thermal aging. The peculiarity that Ni and O coexisted on the surface of the Au-Fe alloy layers, also suggests that Ni diffused to the surface of the Au-Fe alloy layers during the thermal aging process, combined with the oxygen from the atmosphere, and formed oxides. After one minute of etching, the concentration of Ni and O significantly decreased compared to the initial values, indicating that Ni and O only existed on the surface of the electroplated layers.

To investigate the chemical bonding state of the elements present on the surface of the electroplated layers, the XPS spectra of Au (a) and Ni (b) are shown in Fig. 3. The Au (a) on the surface of the electroplated layers was detected as peaks of a metal state, indicating that it was not oxidized on the surface but existed in a metal state. The strength of the Au4f peak

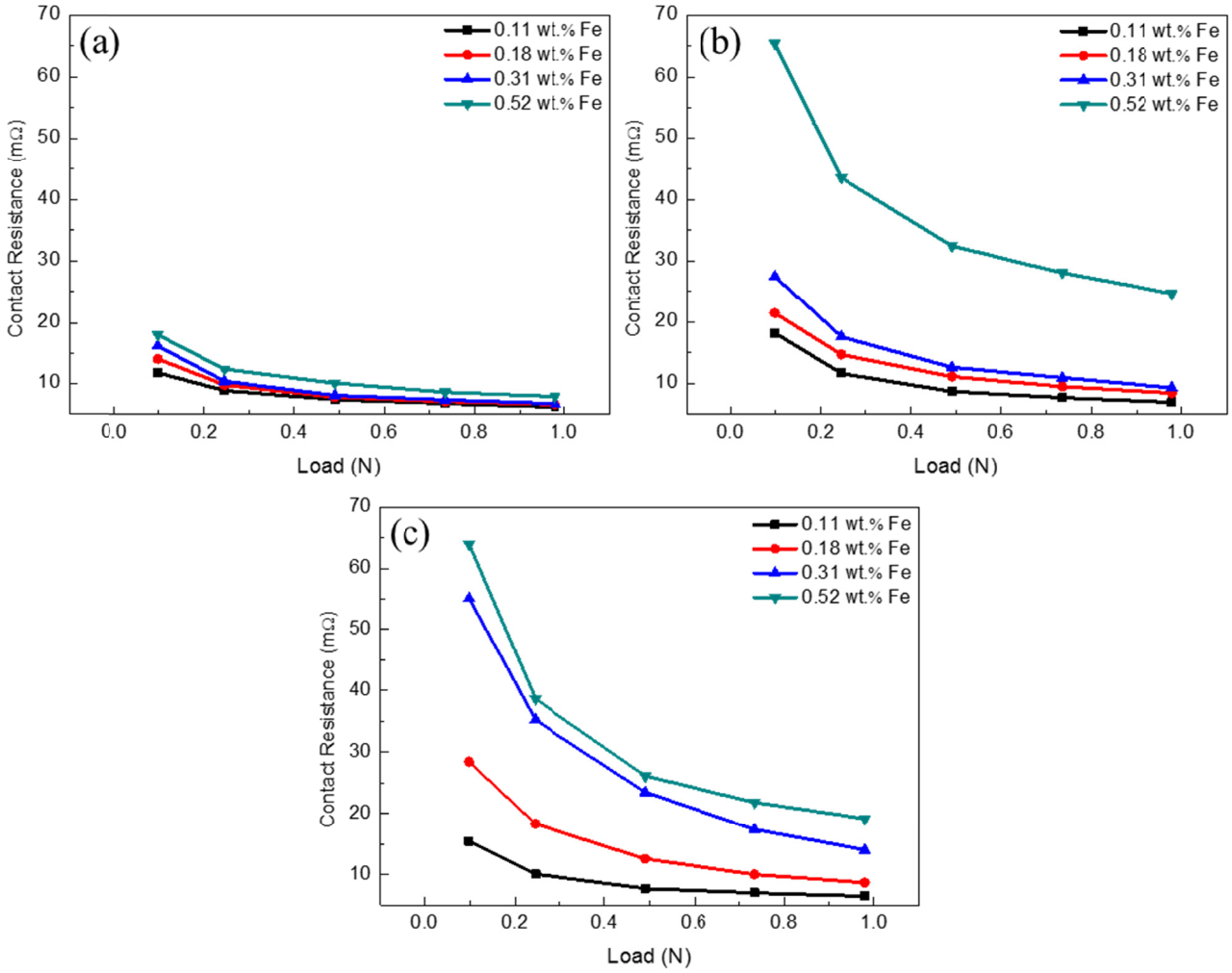

Fig. 1. Contact resistance of electroplated Au-Fe alloy layers (a) immediately after electroplating, (b) after three-minute thermal aging, and (c) after five-minute thermal aging

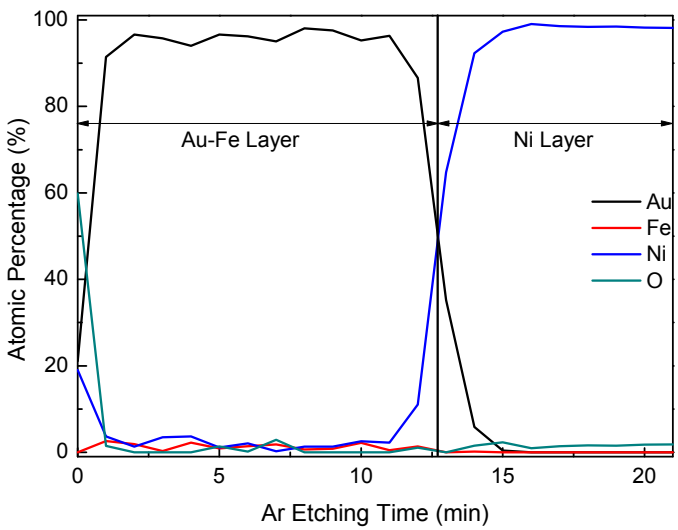

Fig. 2. XPS element depth profile of the electroplated Au-0.18 wt.% Fe alloy layers subjected to five minutes of thermal aging in the atmosphere

intensified as the etching time increased, and the Au content increased towards the interior of the electroplated layers. This is in accordance to the depth profile in Fig. 2. It is observed that Ni (b) exists in the form of oxides, such as NiO and Ni_2O_3 on the surface of the Au-Fe alloy (i.e., at etching time $t = 0$ s). As the etching time increased, the intensity of the nickel oxides decreased. This indicates that the nickel exists in an oxide state on the surface of the electroplated layers, and such oxides exist only on the layer surface. Conversely, the Ni peak of a metal state was not observed when the etching time was 0 s, and was detected 12 and 24 s into the etching process. This is because Ni only exists in the form of oxides on the surface of the electroplated layers. However, it exists in a metal state within the layers, with its content decreasing toward the interior of the electroplated layers.

To investigate the increase in the contact resistance of electroplated Au-Fe alloy layers with an increase in Fe content, a depth-wise component analysis of the layers was conducted using AES. Figure 4 shows the depth profiles of Ni and O, with Fe contents of 0.11 wt.%, 0.31 wt.%, and 0.52 wt.%, respectively. Figure 4(a) presents the depth profile before and after the thermal aging of Au-0.52 wt.% Fe alloy. Here, Ni was absent from the surface of the electroplated Au-Fe alloy layers prior to the thermal aging, but existed in high surface concentrations after the thermal aging process. Similar to the XPS results, the

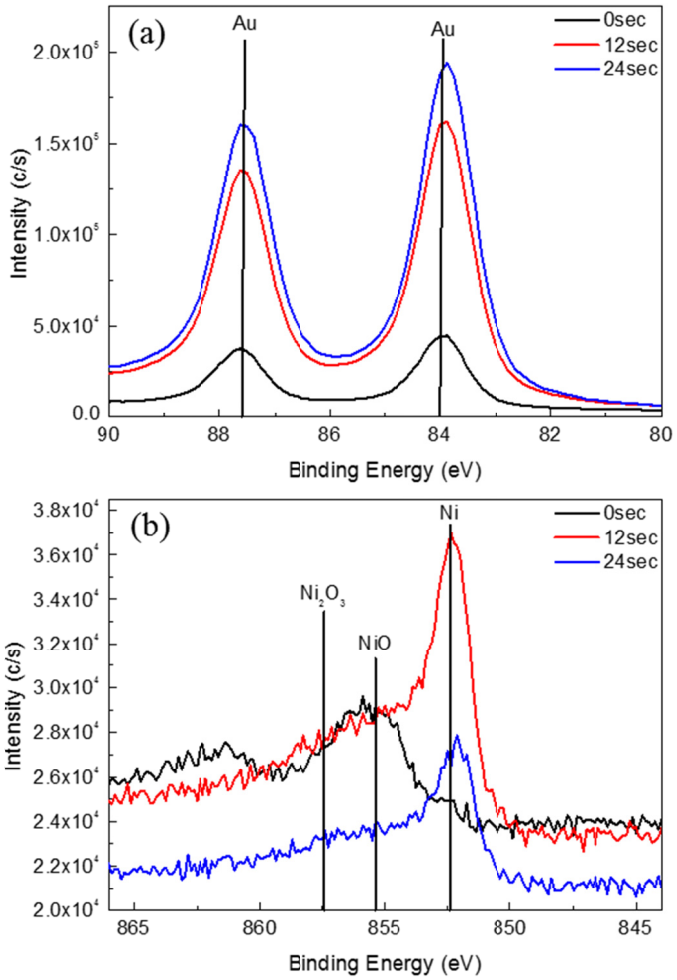

Fig. 3. (a) Au4f (b) Ni2p XPS spectra of the electroplated Au-0.18 wt.% Fe alloy layers subjected to five minutes of thermal aging in the atmosphere

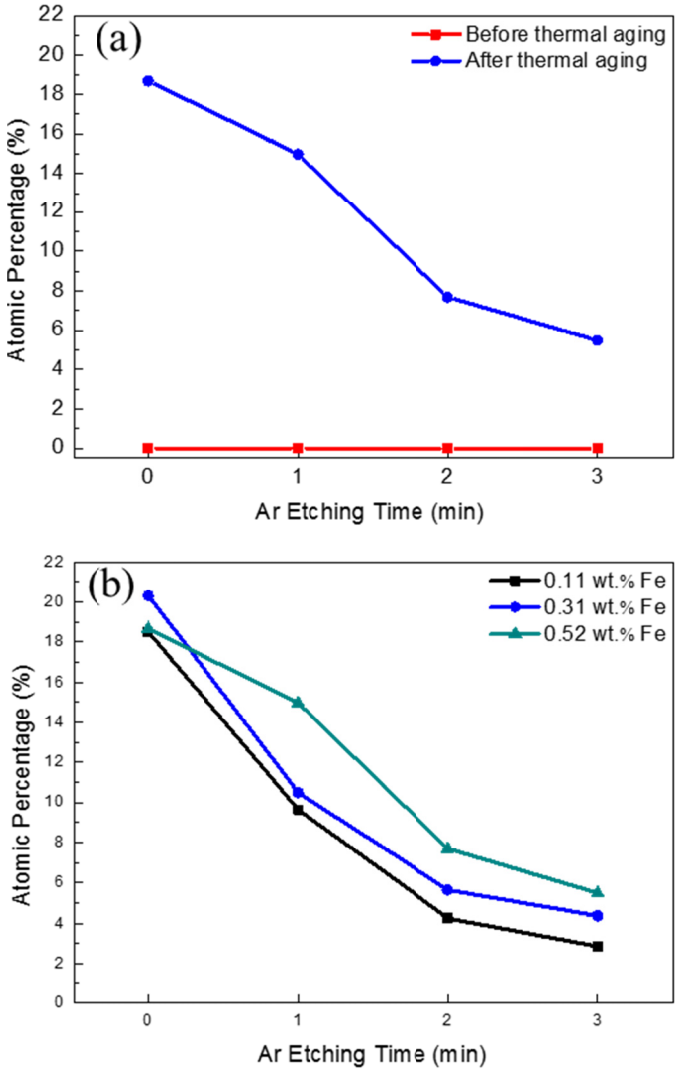

Fig. 4. (a) The AES depth profile of Au- 0.52 wt.% Fe alloy before and after thermal aging for five minutes and (b) AES depth profile of the electroplated Au-Fe alloy layers with the Fe content

amount of Ni present on the surface decreased with etching time. The Ni content (b) along the depth direction increased with an increase in the Fe content, i.e., it is observed that with a rise in the Fe content, the Ni content on the surface of the electroplated layers increases.

For the electroplated Au-0.52 wt.% Fe alloy layers, cross-sectional observations and EDS line analyses were conducted using a FE-TEM. The results are shown in Fig. 5. From the TEM image (a) it is observed that the grain size of the electroplated Au-Fe alloy layers is very small (20-30 nm). The relative grain sizes of electroplated Au-Ni and Au-Co alloy layers are also several tens of nanometers [14]. These grain boundaries are known to act as fast diffusion paths through which Ni atoms from the underlayers can easily disperse during thermal aging [5,15]. In the EDS line analysis of a cross section of the electroplated Au-Fe layers (b), a higher Ni content was detected at the surface of the layers, than within the layers. This observation correlates well with the XPS and AES results (Figs. 2 and 4).

To investigate the increase in Ni content on the surface with the increase in Fe content, XRD analysis was conducted, and the grain size of the electroplated layers was calculated using the Scherrer equation. The results are shown in Fig. 6. The grain size decreases with an increase in the Fe content. i.e., with a decrease in grain size, the area between the grain boundaries increases, creating a fast diffusion path. Therefore, as the Fe content rises, the amount of Ni oxides present on the surface increases, increasing the contact resistance. As the area between grain boundaries increases due to decrease in grain size, the Ni atoms from the nickel underlayers can diffuse through to the surface, thus leading to more nickel oxides forming on the surface of the electroplated Au-Fe alloy layers.

4. Conclusions

The effect of Fe content on the contact resistance of electroplated Au-Fe alloy layers, subject to thermal aging in the atmosphere, was investigated. The contact resistance of the layers after thermal aging significantly increased with a rise in Fe content. As a result of surface analysis through XPS, AES and FE-TEM, it was observed that the Ni from the underlayers

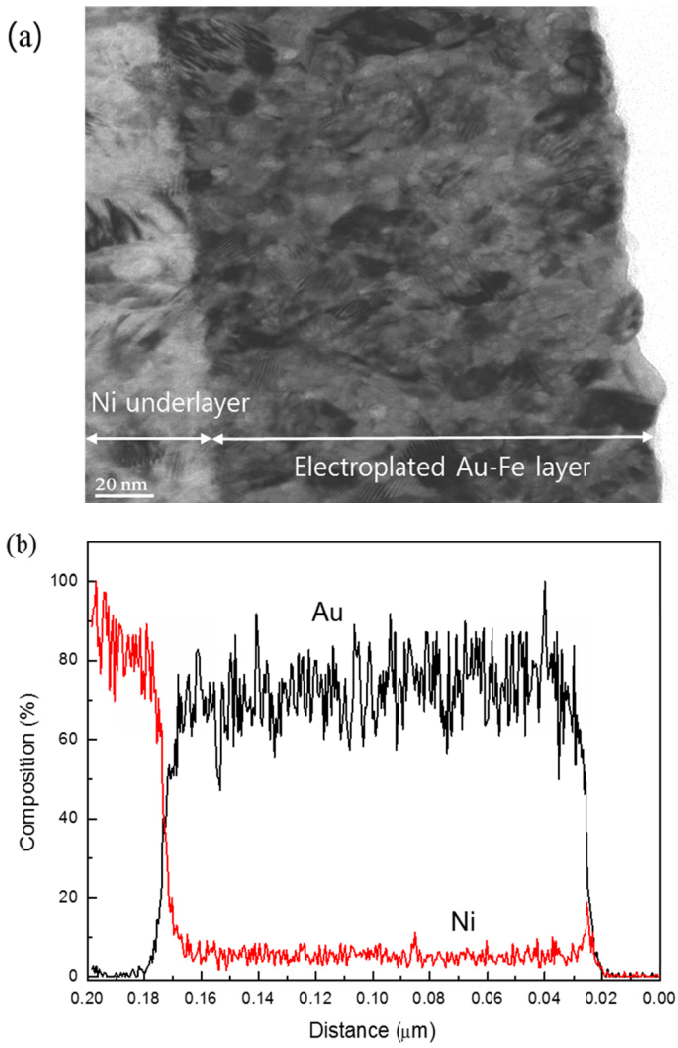

Fig. 5. (a) FE-TEM image and (b) EDS line analysis results of a cross section of the electroplated Au-0.52 wt.% Fe alloy layer after thermal aging for five minutes

diffused to the surface of the electroplated layers by the thermal aging, and reacted with the atmospheric oxygen to form NiO and Ni_2O_3. This led to a significantly increased contact resistance of the electroplated Au-Fe alloy layers post the thermal aging process. The contents of Ni and O on the surface of the electroplated Au-Fe alloy layers were higher with an increase in the Fe content, because the area between grain boundaries, through which Ni can diffuse, increases with a rise in the Fe content. Therefore, it is demonstrated that the contact resistance of electroplated Au-Fe alloy layers, subject to thermal aging, increases with a rise in Fe content

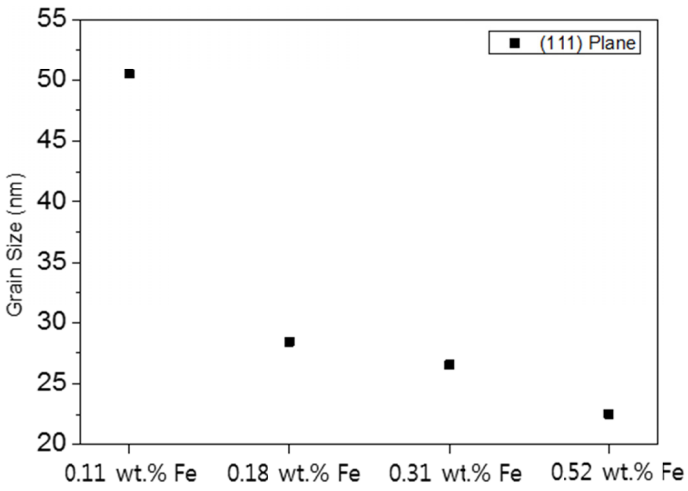

Fig. 6. Grain size of electroplated Au-Fe alloy layers with respect to the Fe content

Acknowledgments

This work was financially supported by Basic Science Research Program through the National Research Foundation of Korea (NRF) funded by the Ministry of Science, ICT and Future Planning (grant No. NRF-2014R1A1A1007848).

REFERENCES

[1] P. Goodman, Gold Bull. **35**, 21 (2002).
[2] I. Christie, B. Cameron, Gold Bull. **27**, 12 (1994).
[3] M. Antler, IEEE Trans. Components, Hybrids, Manuf. Technol. CHMT-10, 420 (1987)
[4] Y. Okinaka, M. Hoshino, Gold Bull. **31**, 3 (1998).
[5] M.R. Pinnel, H G. Tompkins, D.E. Heath, J. Electrochem. Soc. **126** (10), 1798 (1979).
[6] O. Kurtz, J. Barthelmes, R. Ruther, M. Danker, F. Lagorce-Broc, F. Bozsa, D. Brookes, Met. Finish. **109** (5), 19 (2011).
[7] K. Horibe, IEICE Technical Report, EMC91, **61** (1991).
[8] J.W. Lee, I.J. Son, J. Kor. Inst. Surf. Eng. **46** (6), 235 (2013).
[9] H.G Tompkins, M.R. Pinnel, J. Appl. Phys. **48** (7), 3144 (1977).
[10] T.E. Bardy, C.T. Hovland,. J. Vac. Sci. Technol. **18** (2), 339 (1981).
[11] J. Deuber, H.J. Luebke, Plat. Surf. Fin. **69** (7), 55 (1982).
[12] J.K. Bass, H. Fine, GJ. Cisneros, Am. J. Orthod. Dentofacial Orthop. **102**, 280 (1993).
[13] T. Watanabe, J. Sur. Finish. Soc. Jpn. **40**, 280 (1989).
[14] Y. Okinaka, S. Nakahara, J. Electrochem. Soc. **123** (9), 1284 (1976).
[15] M.W. Lee, T.S. Jang, J. Korean Powder Metall. Inst. **23** (6), 432 (2016).